ORGANOMETALLICS

Article

pubs.acs.org/Organometallics

DFT Studies on the Palladium-Catalyzed Dearomatization Reaction between Chloromethylnaphthalene and the Cyclic Amine Morpholine

Hujun Xie,[†,‡] Hong Zhang,[†] and Zhenyang Lin*[,†]

[†]Department of Chemistry, The Hong Kong University of Science and Technology, Clear Water Bay, Kowloon, Hong Kong, People's Republic of China

[‡]Department of Applied Chemistry, Zhejiang Gongshang University, Hangzhou 310035, People's Republic of China

Supporting Information

ABSTRACT: Density functional theory calculations have been performed to investigate the mechanisms of the Pd-catalyzed dearomatization reaction between chloromethylnaphthalene and the cyclic amine morpholine. The calculation results indicate that the reductive elimination leading to the formation of the dearomatic product takes place via an intramolecular C−N bond coupling between the para carbon of an η^3-exo-(naphthyl)methyl ligand and the nitrogen atom of the amide ligand. The free energy barrier is calculated to be only 13.1 kcal/mol, significantly lower than that (37.8 kcal/mol) through the η^3-endo-(naphthyl)methyl intermediate originally thought. For comparison, various C−N coupling reaction pathways leading to the formation of dearomatic and aromatic products have also been examined.

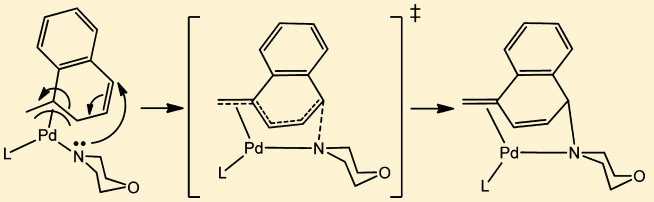

INTRODUCTION

Aromatic compounds possess high thermodynamic stability due to the delocalization of their π bonds. Thus, dearomatization of aromatic compounds is usually difficult to achieve.[1] In 2001, Yamamoto and co-workers[2] reported that palladium(0) complexes catalyzed carbon−carbon coupling reactions of benzyl chlorides with allyltributylstannane to give dearomatization products (eq 1). The reactions are unexpected and

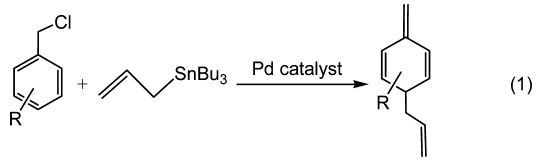

(1)

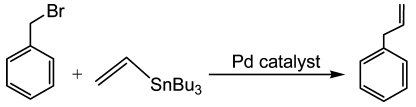

(2)

different from traditional Stille coupling, as displayed in eq 2.[3] To account for the dearomatization reaction, it was originally proposed that the benzyl ligand underwent a rearrangement from an η^3-exo to an η^3-endo coordination mode (Scheme 1). Reductive elimination from an η^3-endo-benzyl intermediate would yield dearomatic products.

In a detailed computational study, Ariafard and Lin reported that the originally proposed η^3-exo to η^3-endo ligand rearrangement is energetically unfavorable.[4] Instead, it was

Scheme 1

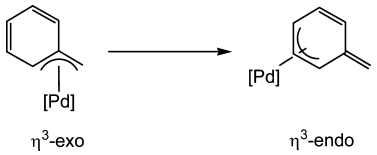

found that a direct C−C bond formation can be achieved from the η^3-exo intermediate to give a dearomatization product via coupling of the C-3 terminus of the η^1-allyl ligand with the para carbon of the η^3-exo-benzyl ligand (Scheme 2). The key feature

Scheme 2

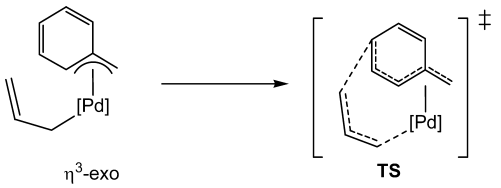

of the new proposed mechanism is related to the ability of the allyl ligand to facilitate a sigmatropic-type rearrangement (**TS** in Scheme 2). A similar sigmatropic-type rearrangement has also been found in a very recently reported theoretical study on the palladium-catalyzed dearomatization reaction of chloromethylnaphthalene and allenyltributylstannane.[5]

Received: December 16, 2012
Published: April 10, 2013

Downloaded via XIAMEN UNIV on July 19, 2018 at 06:37:38 (UTC).
See https://pubs.acs.org/sharingguidelines for options on how to legitimately share published articles.

© 2013 American Chemical Society

dx.doi.org/10.1021/om301215a | Organometallics 2013, 32, 2336−2343

Recently, Bao and co-workers[6] reported the amination reactions of chloromethylnaphthalene and chloromethylanthracene derivatives with various amines catalyzed by $Pd(PPh_3)_4$ complexes (eq 3). The results showed that regioselective

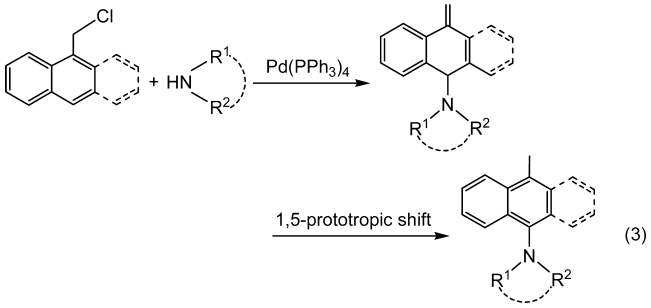

(3)

amination reactions occur to first give dearomatization para-aminated products, and then a 1,5-prototropic shift occurs to yield aromatic amines. Preliminary experimental results led the authors to propose the mechanism shown in Scheme 3 using morpholine as the substrate, which consists of oxidative addition, rearrangement, ligand substitution, and reductive elimination steps. The rearrangement involves a change in the coordination mode of the η^3-(naphthyl)methyl ligand from an η^3-exo-(naphthyl)methyl to an η^3-endo-(naphthyl)methyl.[2]

A couple of interesting questions arise when we compare the two dearomatization reactions (eqs 1 and 3). As mentioned above, an allyl ligand is able to facilitate a sigmatropic-type rearrangement (Scheme 2). Is an amide ligand (e.g., the amide ligand of **3** in Scheme 3) also able to promote a similar type of rearrangement as an allyl ligand does (shown in Scheme 2)? Or with an amide ligand (not an allyl ligand), does the reaction have to occur with a mechanism involving an η^3-exo- to η^3-endo-(naphthyl)methyl rearrangement, as shown in Scheme 3, in order to achieve dearomatization? To answer these questions, we carried out DFT calculations by examining structural and energetic aspects of various possible reaction pathways.

Scheme 3

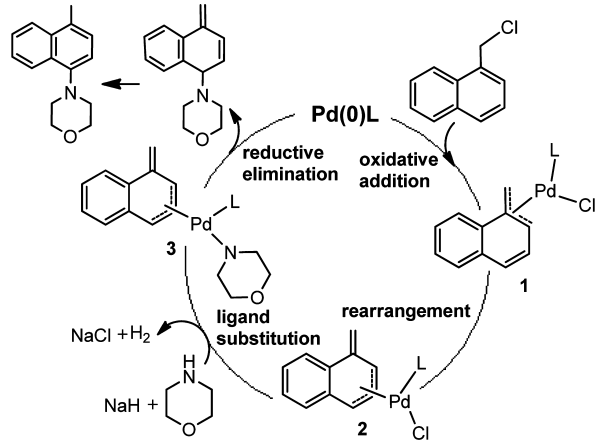

COMPUTATIONAL DETAILS

Geometry optimizations for all species studied in this work have been performed by means of a hybrid Becke3LYP (B3LYP) method,[7] which was adopted in our previous work and in other literature papers on mechanistic studies of Pd-catalyzed reactions.[8] The 6-31g(d) basis set was chosen to describe the C, O, N, and H atoms, and the effective core potentials of Hay and Wadt with double-ζ valence basis set (LanL2DZ) were used for the Pd and P atoms.[9] Polarization functions were also added: $Pd(\zeta_f) = 1.472$[10] and $P(\zeta_d) = 0.340$.[11] For each optimized species, vibrational frequency analyses have been carried out to obtain free energies at 298.15 K and identify all of the stationary points as minima (zero imaginary frequency) or transition states (one imaginary frequency) on the potential energy surfaces (PES). Intrinsic reaction coordinate (IRC) calculations were also performed to confirm that the transition states indeed connect two corresponding minima.[12] To reduce the computational costs, the triphenylphosphine (PPh_3) ligand, employed experimentally, was replaced by phosphine (PH_3), and the reliability of the models will be further discussed in a separate section by providing a few examples with calculations on the realistic PPh_3 ligand using the ONIOM approach.[4,13] To estimate the degree of aromaticity of the (naphthyl)methyl ligand, nucleus-independent

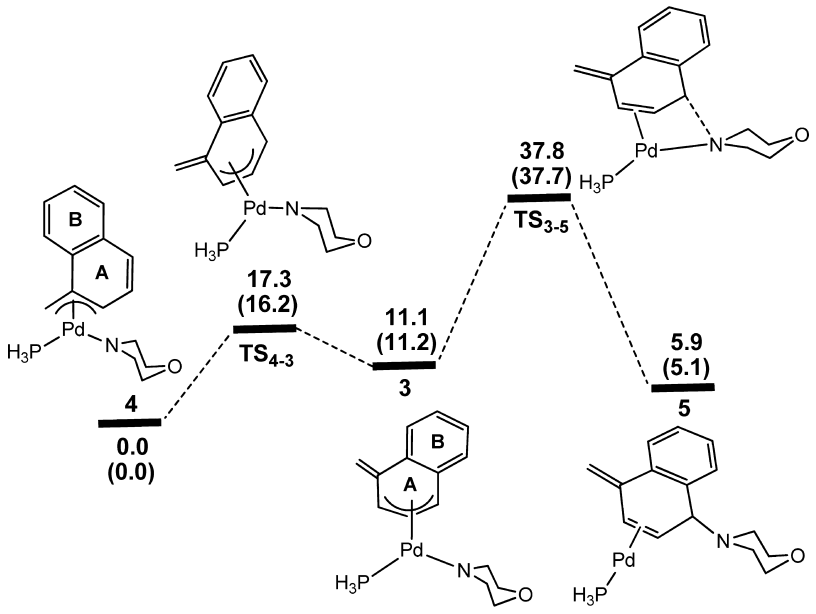

Figure 1. Free energy profiles calculated for the η^3-exo- to η^3-endo-(naphthyl)methyl rearrangement followed by reductive elimination to give the dearomatization product molecule as a ligand. The relative free energies and relative energies (in parentheses) are given in kcal/mol.

dx.doi.org/10.1021/om301215a | Organometallics 2013, 32, 2336−2343

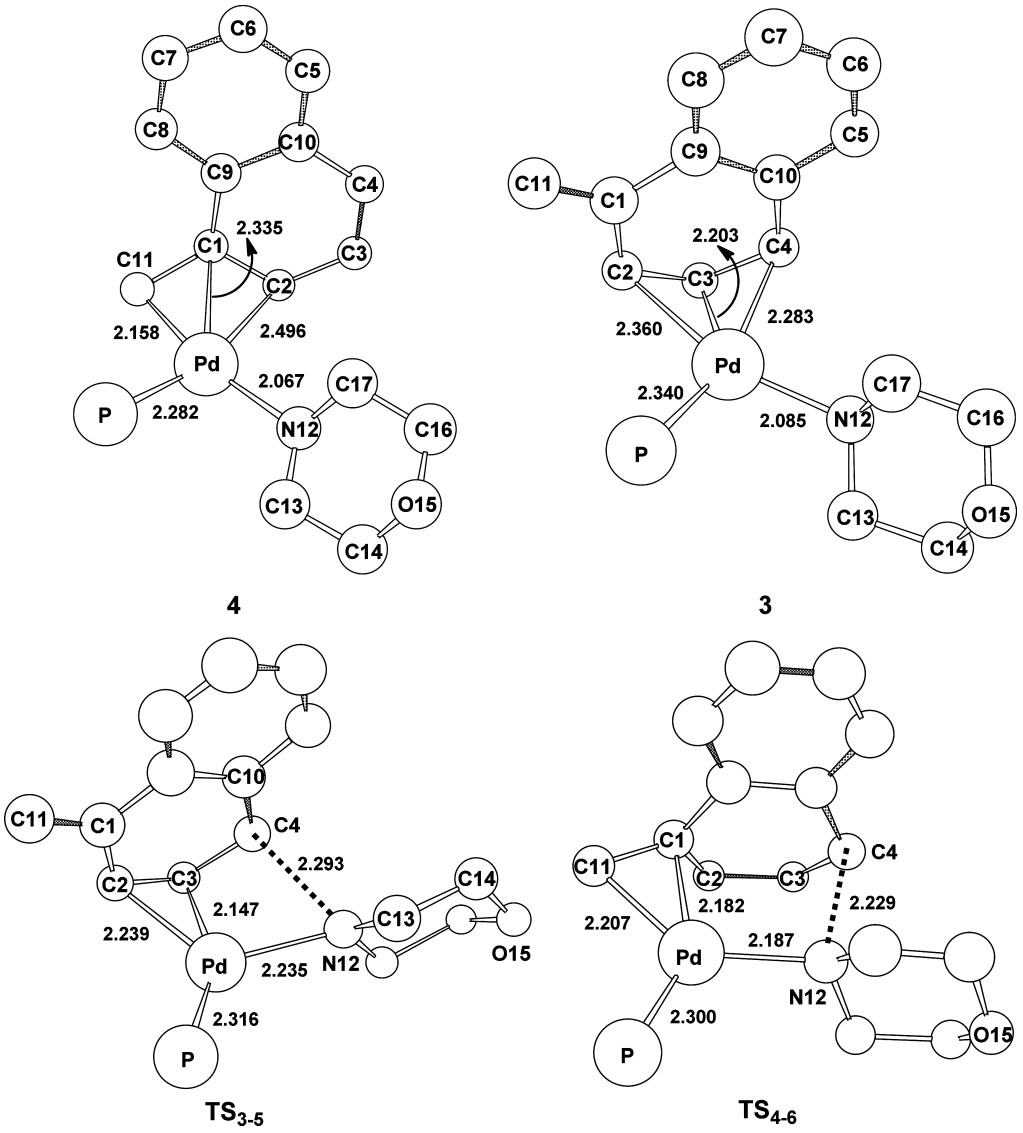

Figure 2. Optimized structures with selected bond lengths (Å) for the species **4**, **3**, TS_{3-5}, and TS_{4-6}. All hydrogen atoms are omitted for clarity.

chemical shift (NICS)[14] calculations were performed using the GIAO[15] method at the same theoretical level as optimization.

In the ONIOM calculations, a two-layer model (B3LYP/Gen:HF/3-21g)[16] was employed with the real PPh_3 ligand for two important steps (vide infra). The phenyl groups on the phosphine ligand were treated as the second layer, while the rest were treated as the first layer. Gen represents the basis sets mentioned above. In addition, single-point energy calculations with the M05-2X[17] functional have also been carried out to test the B3LYP functional used in this work. All calculations were performed with the Gaussian 09 software package.[18]

In all of the figures that contain potential energy profiles, calculated relative free energies (kcal/mol) and relative energies (in parentheses, kcal/mol) are presented. In this paper, relative free energies are used to analyze the reaction mechanism.

RESULTS AND DISCUSSION

Dearomatization Reaction Mechanism. We first examined the reaction mechanism proposed by Bao and co-workers by considering the η^3-exo- to η^3-endo-(naphthyl)methyl rearrangement followed by reductive elimination to give the dearomatization product molecule as a ligand (Scheme 3). Figure 1 shows the free energy profiles calculated for the rearrangement and reductive elimination steps, and Figure 2 shows the key structures and transition states with selected structural parameters. From Figure 1, we can see that an overall free energy barrier of 37.8 kcal/mol was calculated on the basis of this proposed mechanism, suggesting that the pathway via the η^3-exo- to η^3-endo-(naphthyl)methyl rearrangement is energetically very unfavorable.

The η^3-endo-(naphthyl)methyl structure **3** is less stable by 11.1 kcal/mol than the η^3-exo-(naphthyl)methyl structure **4**, a result related to the fact that the structure **3** has a lower aromaticity. Nucleus-independent chemical shift (NICS) values were calculated for the relevant phenyl rings of two structures to provide support to the argument given here. The NICS(0) values were computed from the center of the A ring (see Figure 1 for the labels of A and B rings) in the (naphthyl)methyl ligand, and the NICS(1) values were derived at a point 1.0 Å away from the center of the A ring, in a direction perpendicular to the plane of the A ring and opposite to the palladium center. The calculated NICS(1) [NICS(0)] values are −7.4 [−4.9] and −2.0 [−1.0] for the structures **4** and **3**, respectively.

In view of the energetically highly unfavorable pathway associated with the proposed mechanism shown in Scheme 3,[6] we therefore examined the direct coupling pathway mentioned

dx.doi.org/10.1021/om301215a | *Organometallics* 2013, 32, 2336−2343

Scheme 4

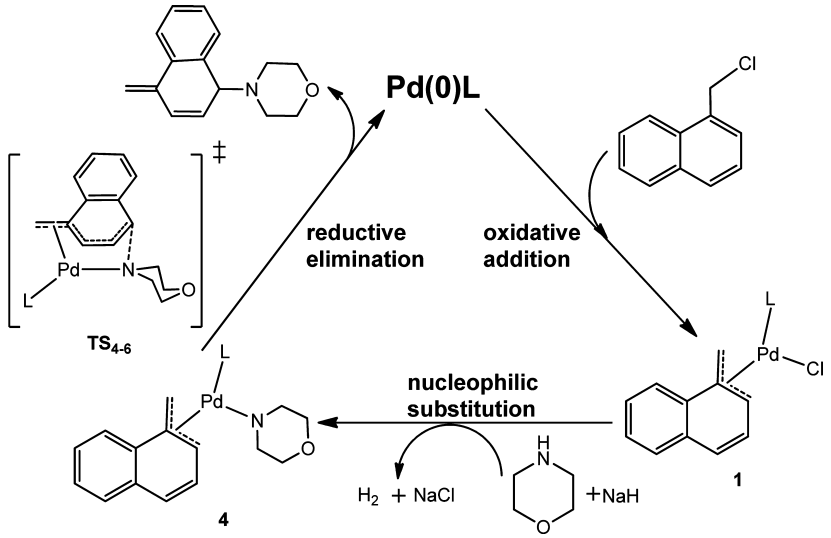

in the Introduction and shown in Scheme 4 involving a sigmatropic-type rearrangement. Figure 3 shows the free energy profiles calculated for the newly proposed pathway. Remarkably, the free energy barrier is as low as 13.1 kcal/mol. The reductive elimination occurs directly from **4** via $\mathbf{TS}_{46}$, having an intramolecular C−N bond coupling between the para carbon of the η^3-exo-(naphthyl)methyl and nitrogen of the amide ligand.

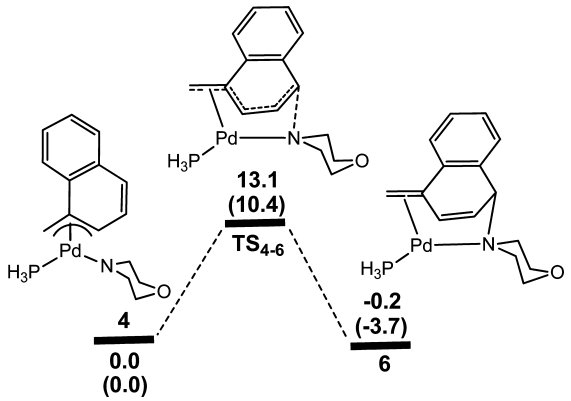

Figure 3. Free energy profiles calculated for the reductive elimination from complex **4** on the basis of the reaction mechanism shown in Scheme 4. The relative free energies and relative energies (in parentheses) are given in kcal/mol.

Pathways Leading to Formation of Other Dearomatic Products. In addition to the favorable dearomatic pathway mentioned above, we also consider six other possible coupling pathways leading to formation of other dearomatic products (starting from complex **4**). Figure 4 shows the free energy profiles calculated for these pathways, which correspond to the intramolecular C−N bond couplings of the amide ligand with different ring carbons of the η^3-exo-(naphthyl)methyl ligand, leading to the formation of other dearomatic products. Comparing Figure 4 with Figure 3, we can see that the smallest free energy barrier (17.1 kcal/mol) is calculated for the pathway having C−N coupling of the amide ligand with the ortho ring carbon (C2), which is still higher than the free energy barrier calculated for the pathway shown in Figure 3. Other transition states, i.e. 31.1 ($\mathbf{TS}_{48}$), 41.9 ($\mathbf{TS}_{9\text{-}10}$), 60.4 ($\mathbf{TS}_{4\text{-}11}$), 34.3 ($\mathbf{TS}_{4\text{-}12}$), and 47.3 kcal/mol ($\mathbf{TS}_{4\text{-}13}$), are significantly higher in free energy than that of $\mathbf{TS}_{46}$ (13.1 kcal/mol). Judging from the barriers calculated for the six pathways, the para carbon is the most favorable position of the η^3-exo-(naphthyl)methyl to undergo direct coupling with nitrogen of the amide ligand, in good agreement with the previous experimental observations.[6]

Pathways of Coupling of the Amide Ligand with the (Naphthyl)methyl Methyl Carbon Leading to the Formation of Aromatic Products. We then examined the possible pathways for direct coupling of the amide ligand with the (naphthyl)methyl carbon to form the usually expected aromatic products. Figure 5 shows the free energy profiles calculated for four direct coupling pathways to give the corresponding precursor complexes **14**, **16**, **18**, and **20**. The barriers of these pathways are calculated to be 15.5 ($\mathbf{TS}_{4\text{-}14}$), 22.4 ($\mathbf{TS}_{15\text{-}16}$), 29.7 ($\mathbf{TS}_{17\text{-}18}$), and 29.6 kcal/mol ($\mathbf{TS}_{19\text{-}20}$), respectively. Consistent with the experimental observations, all the direct coupling transition states are higher in energy than that calculated for the most favorable transition state $\mathbf{TS}_{46}$ (13.1 kcal/mol, Figure 3) leading to the formation of the experimentally observed coupling dearomatic product.

As seen from the free energy profiles shown in Figures 3 and 5, the precursor complexes **14**, **16**, **18**, and **20**, possessing aromatic products as a ligand, are much more stable than the precursor complex **6**, possessing dearomatic product as a ligand. It is noted that the relative stabilities of the coupling products that act as ligands play an important role in the relative stabilities of these precursor complexes. The assumption is confirmed by the estimation of the free energy difference between the aromatic and dearomatic products to be 24.6 kcal/mol (Scheme 5). Therefore, we can conclude that the direct coupling via the transition state $\mathbf{TS}_{4\text{-}6}$ is kinetically more favorable but thermodynamically less favorable.

The most favorable transition state $\mathbf{TS}_{4\text{-}6}$ (13.1 kcal/mol, Figure 3) leading to the formation of the dearomatic product is only 2.4 kcal/mol lower than the most favorable direct coupling transition state $\mathbf{TS}_{4\text{-}14}$. Furthermore, complexes **4** and **6** have similar stabilities. Here, one may argue that the formation of complex **6** has no significant preference in comparison with the formation of the complex **14**, if the reversibility of **6** to **4** is considered. Therefore, we examined the further conversion of

dx.doi.org/10.1021/om301215a | Organometallics 2013, 32, 2336−2343

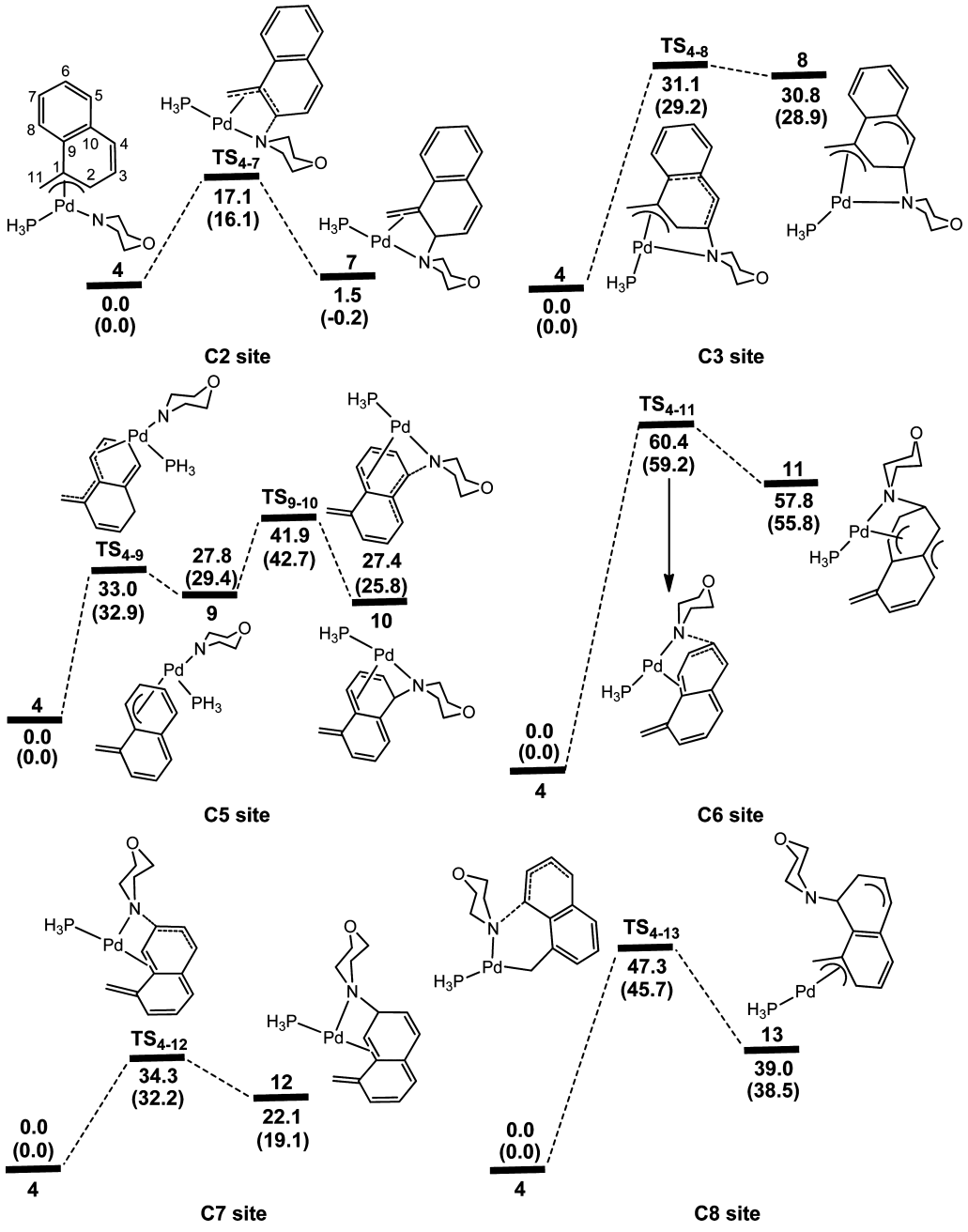

Figure 4. Free energy profiles calculated for the reductive elimination in complex **4** leading to formation of other dearomatic products. The relative free energies and relative energies (in parentheses) are given in kcal/mol.

complex **6** to other much more stable species and eventually to the experimentally observed isomerized aromatic product **III** (Scheme 5) via a 1,5-prototropic shift. Our calculations suggested that the 1,5-prototropic shift can be facilitated by sodium amide, which was formed from NaH and morpholine. Sodium amide first abstracts the proton bonded to the morpholine-substituted carbon from the dearomatic product **II** and then passes it to the terminal methylene carbon to give the experimentally observed product **III**. The whole 1,5-prototropic shift process is very thermodynamically favorable and very facile with barriers of smaller than 10 kcal/mol (see the Supporting Information). These results indicate that the reversibility of **6** to **4** does not occur.

Similarity between Amide and Allyl Ligands. As shown in the Introduction, our previous calculations[4] demonstrated that the allyl ligand could facilitate the reductive elimination reaction for the formation of dearomatic products via the coupling of the C-3 terminus of the η^1-allyl ligand with the para carbon of the η^3-exobenzyl ligand (Scheme 2). On the basis of the above DFT calculation results, we can draw an analogy between an amide ligand and an η^1-allyl ligand. Scheme 6 illustrates the similarity between them in the reductive elimination step, in which both of the ligands have an available electron pair ready to interact with the para carbon. For an allyl ligand (Scheme 6a), the reductive elimination occurs via the attack of the π electron pair of the terminal double bond at the para carbon of the benzyl ligand, whereas the nitrogen atom of the amide ligand can provide the lone electron pair to attack the para carbon of the (naphthyl)methyl ligand (Scheme 6b),

dx.doi.org/10.1021/om301215a | *Organometallics* 2013, 32, 2336−2343

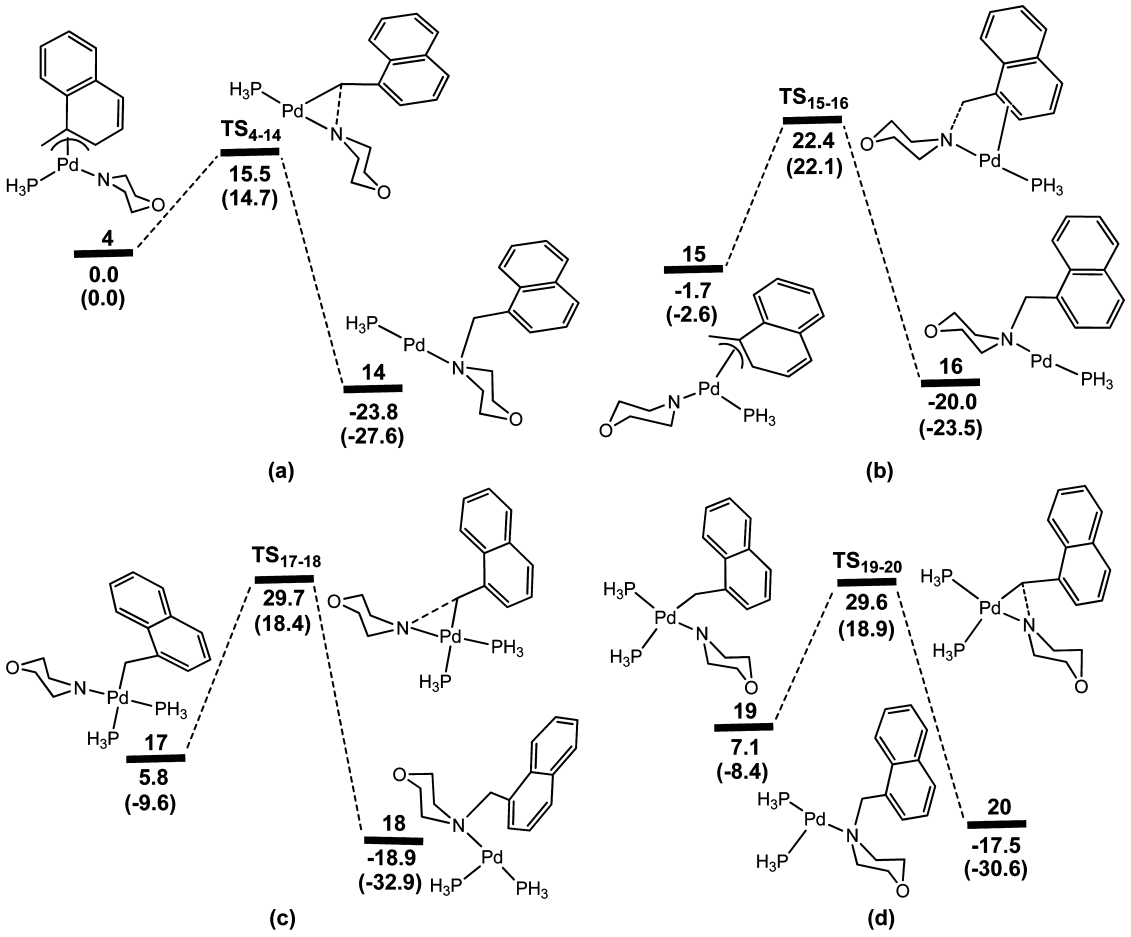

Figure 5. Free energy profiles calculated for four other possible reductive elimination reactions for the formation of expected aromatic products. The relative free energies and relative energies (in parentheses) are given in kcal/mol.

Scheme 5

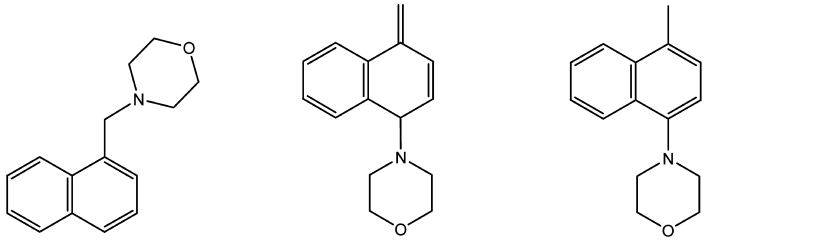

which makes the dearomatization reactions kinetically favorable.

ONIOM Calculations for the Reductive Elimination Step. To take the steric effects into account, we carried out two-layer ONIOM calculations with the real PPh_3 ligand for the **4** → $\mathbf{TS}_{4\text{-}6}$ and **4** → $\mathbf{TS}_{4\text{-}17}$ steps. The **4** → $\mathbf{TS}_{4\text{-}6}$ step gives the dearomatization product as a ligand, while the **4** → $\mathbf{TS}_{4\text{-}14}$ step is the lowest energy pathway giving the direct (normally expected) coupling product. The ONIOM calculation results show that the steric bulk of the PPh_3 ligand has nearly no effect on the important steps calculated. In the PH_3 model calculations, the barriers in terms of electronic energies from **4** → $\mathbf{TS}_{4\text{-}6}$ and from **4** → $\mathbf{TS}_{4\text{-}17}$ are calculated to be 10.4 and 14.7 kcal/mol, respectively. In the PPh_3 calculations, the barriers from **4** → $\mathbf{TS}_{4\text{-}6}$ and from **4** → $\mathbf{TS}_{4\text{-}17}$ are calculated to be 10.3 and 16.5 kcal/mol, respectively. In addition, single-point calculations with the M05-2X functional on the basis of the ONIOM-optimized structures for the barriers from **4** → $\mathbf{TS}_{4\text{-}6}$ and from **4** → $\mathbf{TS}_{4\text{-}17}$ were calculated to be 10.4 and 15.8 kcal/mol, respectively. The results are consistent with those from the B3LYP calculations. The calculation results also indicate that the geometry around the palladium center in these ONIOM-optimized structures does not change much with respect to those obtained from the model calculations (see the Supporting Information for more details). The negligible effect of the steric bulk is related to the fact that the Pd species usually have low coordination numbers.

dx.doi.org/10.1021/om301215a | *Organometallics* 2013, 32, 2336−2343

Scheme 6. Comparison of Allyl and Amide Ligands in the Reductive Elimination Steps

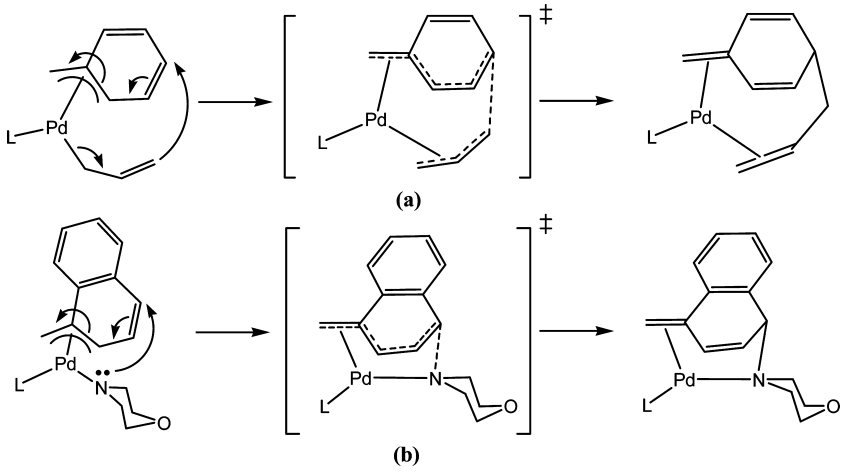

CONCLUSIONS

The dearomatization reactions of chloromethylnaphthalene with the cyclic amine morpholine catalyzed by Pd(0) complexes have been investigated with the aid of density functional theory calculations. On the basis of DFT calculations, we found that the dearomatization reaction mechanism involves an intramolecular C−N bond coupling between the para carbon of an η^3-exo-(naphthyl)methyl ligand and the nitrogen atom of the amide ligand.

Various coupling (reductive elimination) pathways leading to formation of other dearomatic products were also examined by considering intramolecular C−N bond couplings of the amide ligand with different ring carbons of the η^3-exo-(naphthyl)-methyl ligand. These couplings were calculated to be kinetically less favorable than the coupling between the para carbon of the η^3-exo-(naphthyl)methyl and the nitrogen atom of the amide ligand. The direct coupling of the (naphthyl)methyl carbon with the amide ligand to form the usually expected aromatic products was also found to be kinetically less favorable.

We have also illustrated the similarity between allyl and amide ligands in the reductive elimination step, in which both of the ligands have an available electron pair ready to interact with the para carbon. For an allyl ligand, the reductive elimination takes place via the attack of the π electron pair of the terminal double bond at the para carbon of the benzyl ligand, whereas for an amide ligand, the lone pair on the nitrogen atom of the amide ligand attacks the para carbon of the (naphthyl)methyl ligand, making the dearomatization reactions kinetically favorable.

ASSOCIATED CONTENT

Supporting Information

Text giving the complete ref 18 and tables giving the Cartesian coordinates for all of the calculated structures. This material is available free of charge via the Internet at http://pubs.acs.org.

AUTHOR INFORMATION

Corresponding Author

*E-mail for Z.L.: chzlin@ust.hk.

Notes

The authors declare no competing financial interest.

ACKNOWLEDGMENTS

This work was supported by the Research Grants Council of Hong Kong (HKUST603711) and the National Natural Science Foundation of China (21203166).

REFERENCES

(1) (a) Barner, B. A.; Meyers, A. I. *J. Am. Chem. Soc.* **1984**, *106*, 1865. (b) Maruoka, K.; Ito, M.; Yamamoto, H. *J. Am. Chem. Soc.* **1995**, *117*, 9091. (c) Berger, R.; Ziller, J. W.; Vranken, D. L. V. *J. Am. Chem. Soc.* **1998**, *120*, 841. (d) Schultz, A. G. *Chem. Commun.* **1999**, 1263. (e) Pape, A. R.; Kaliappan, K. P.; Kündig, E. P. *Chem. Rev.* **2000**, *100*, 2917. (f) Chordia, M. D.; Harman, W. D. *J. Am. Chem. Soc.* **2000**, *122*, 2725. (g) Graham, P. M.; Meiere, S. H.; Sabat, M.; Harman, W. D. *Organometallics* **2003**, *22*, 4364. (h) Ding, F.; Valahovic, M. T.; Keane, J. M.; Anstey, M. R.; Sabat, M.; Trindle, C. O.; Harman, W. D. *J. Org. Chem.* **2004**, *69*, 2257. (i) Fernandez, I.; Gonzalez, J.; Lopez-Ortiz, F. *J. Am. Chem. Soc.* **2004**, *126*, 12551. (j) Keane, J. M.; Harman, W. D. *Organometallics* **2005**, *24*, 1786. (k) Delafuente, D. A.; Myers, W. H.; Sabat, M.; Harman, W. D. *Organometallics* **2005**, *24*, 1885. (l) Zhu, J.; Grigoriadis, N. P.; Lee, J. P.; Porco, J. A., Jr. *J. Am. Chem. Soc.* **2005**, *127*, 9342. (m) Jantunen, K. C.; Scott, B. L.; Hay, P. J.; Gordon, J. C.; Kiplinger, J. L. *J. Am. Chem. Soc.* **2006**, *128*, 6322. (n) Zhou, L.; Wu, L. Z.; Zhang, L. P.; Tung, C. H. *Organometallics* **2006**, *25*, 1707. (o) Monje, P.; Grana, P.; Paleo, M. R.; Sardina, F. J. *Org. Lett.* **2006**, *8*, 954. (p) Pigge, F. C.; Coniglio, J. J.; Dalvi, R. *J. Am. Chem. Soc.* **2006**, *128*, 3498.

(2) Bao, M.; Nakamura, H.; Yamamoto, Y. *J. Am. Chem. Soc.* **2001**, *123*, 759.

(3) Milstein, D.; Stille, J. K. *J. Am. Chem. Soc.* **1979**, *101*, 4992.

(4) Ariafard, A.; Lin, Z. Y. *J. Am. Chem. Soc.* **2006**, *128*, 13010.

(5) Ren, Y.; Jia, J.; Liu, W.; Wu, H.-S. *Organometallics* **2013**, *32*, 52.

(6) Zhang, S.; Wang, Y.; Feng, X. J.; Bao, M. *J. Am. Chem. Soc.* **2012**, *134*, 5492.

(7) (a) Becke, A. D. *J. Chem. Phys.* **1993**, *98*, 5648. (b) Lee, C.; Yang, W.; Parr, R. G. *Phys. Rev. B* **1988**, *37*, 785. (c) Becke, A. D. *J. Chem. Phys.* **1993**, *98*, 1372. (d) Becke, A. D. *Phys. Rev. B* **1988**, *38*, 3098.

(8) (a) Lam, K. C.; Marder, T. B.; Lin, Z. Y. *Organometallics* **2010**, *29*, 1849. (b) Xue, L. Q.; Lin, Z. Y. *Chem. Soc. Rev.* **2010**, *39*, 1692. (c) Yu, H. Z.; Fu, Y.; Guo, Q. X.; Lin, Z. Y. *Organometallics* **2009**, *28*, 4507. (d) Bai, T.; Xue, L. Q.; Xue, P.; Zhu, J.; Sung, H. H. Y.; Ma, S. M.; Wiliams, I. D.; Lin, Z. Y.; Jia, G. C. *Organometallics* **2008**, *27*, 2614. (e) Zheng, W. X.; Ariafard, A.; Lin, Z. Y. *Organometallics* **2008**, *27*, 246. (f) Lam, K. C.; Marder, T. B.; Lin, Z. Y. *Organometallics* **2007**, *26*, 758. (g) Tang, S. Y.; Guo, Q. X.; Fu, Y. *Chem. Eur. J.* **2011**, *49*, 13866. (h) Perez-Rodriguez, M.; Braga, A. A. C.; de Lera, A. R.; Maseras, F.; Alvarez, R.; Espinet, P. *Organometallics* **2010**, *29*, 4983. (i) Surawatanawong, P.; Hall, M. B. *Organometallics* **2008**, *27*, 6222.

(9) (a) Check, C. E.; Faust, T. O.; Bailey, J. M.; Wright, B. J.; Gilbert, T. M.; Sunderlin, L. S. *J. Phys. Chem. A* **2001**, *105*, 8111. (b) Hay, P. J.; Wadt, W. R. *J. Chem. Phys.* **1985**, *82*, 299.
(10) Ehlers, A. W.; Bohme, M.; Dapprich, S.; Gobbi, A.; Hollwarth, A.; Jonas, V.; Kohler, K. F.; Stegmann, R.; Veldkamp, A.; Frenking, G. *Chem. Phys. Lett.* **1993**, *208*, 111.
(11) Huzinaga, S. *Gaussian Basis Sets for Molecular Calculations*; Elsevier Science: Amsterdam, 1984.
(12) (a) Fukui, K. *J. Phys. Chem.* **1970**, *74*, 4161. (b) Fukui, K. *Acc. Chem. Res.* **1981**, *14*, 363.
(13) (a) Legault, C. Y.; Garcia, Y.; Merlic, C. A.; Houk, K. N. *J. Am. Chem. Soc.* **2007**, *129*, 12664. (b) Ariafard, A.; Lin, Z. Y. *Organometallics* **2006**, *25*, 4030. (c) Bai, T.; Zhu, J.; Xue, P.; Sung, H. H. Y.; Williams, I. D.; Ma, S. M.; Lin, Z. Y.; Jia, G. C. *Organometallics* **2007**, *26*, 5581. (d) Lam, K. C.; Lin, Z. Y.; Marder, T. B. *Organometallics* **2007**, *26*, 3149. (e) Zhang, L.; Dang, L.; Wen, T. B.; Sung, H. H. Y.; Williams, I. D.; Lin, Z. Y.; Jia, G. C. *Organometallics* **2007**, *26*, 2849. (f) Leung, C. W.; Zheng, W. X.; Zhou, Z. Y.; Lin, Z. Y.; Lau, C. P. *Organometallics* **2008**, *27*, 4957. (g) Hung, W. Y.; Liu, B.; Shou, W. G.; Wen, T. B.; Shi, C.; Sung, H. H. Y.; Williams, I. D.; Lin, Z. Y.; Jia, G. C. *J. Am. Chem. Soc.* **2011**, *133*, 18350.
(14) Schleyer, P. v. R.; Maerker, C.; Dransfeld, A.; Jiao, H.; van Eikema Hommes, N. J. R. *J. Am. Chem. Soc.* **1996**, *118*, 6317.
(15) Wolinski, K.; Hinton, J. F.; Pulay, P. *J. Am. Chem. Soc.* **1990**, *112*, 8251.
(16) (a) Dapprich, S.; Komaromi, I.; Byun, K. S.; Morokuma, K.; Frisch, M. J. *J. Mol. Struct. (THEOCHEM)* **1999**, *462*, 1. (b) Vreven, T.; Morokuma, K. *J. Comput. Chem.* **2000**, *21*, 1419. (c) Ananikov, V. P.; Szilagyi, R.; Morokuma, K.; Musaev, D. G. *Organometallics* **2005**, *24*, 1938.
(17) (a) Zhao, Y.; Schultz, N. E.; Truhlar, D. G. *J. Chem. Theory Comput.* **2006**, *2*, 364. (b) Zhao, Y.; Truhlar, D. G. *Acc. Chem. Res.* **2008**, *41*, 157.
(18) Frisch, M. J.; et al. *Gaussian 09, Revision A.1*; Gaussian Inc., Wallingford, CT, 2009.